Emergent Materials (2024) 7:509–519
https://doi.org/10.1007/s42247-023-00613-w

ORIGINAL ARTICLE

Improved properties and salt rejection of polysulfone membrane by incorporation of hydrophilic cobalt-doped ZnO nanoparticles

Muneer M. Ba-Abbad[1] · Nafis Mahmud[1] · Abdelbaki Benamor[1] · Ebrahim Mahmoudi[2] · Mohd S. Takriff[3] · Abdul Wahab Mohammad[3]

Received: 11 October 2023 / Accepted: 13 December 2023 / Published online: 5 January 2024

Abstract
In this study, the nanoparticles (NPs) of ZnO and Co^{2+} ions doped ZnO (doped ZnO) were incorporated into a matrix of polysulfone (PSf) membranes to enhance their surface properties prepared using a simple wet phase inversion technique. The hybrid PSf membranes were fabricated with 0.5 wt. % of ZnO and doped ZnO NPs. These membranes were characterized using XRD, TGA, FESEM-EDX, and salt rejection performance. The hydrophilicity of PSf membranes was improved by adding of ZnO and doped ZnO NPs which showed a decrease in contact angle values from 82° to 62° with an increased flux with water. Among the prepared membranes, doped ZnO NPs showed the highest salt rejection for both sodium chloride (NaCl) and sodium sulfate (Na_2SO_4) compared to pure PSf and PSf with ZnO NPs which confirm the improvement contact angle and water permeability. Overall, the results of this study showed that embedding a small amount of Co^{2+} ions doped ZnO NPs with PSf has significant potential to be applied in industrial-scale membrane applications.

Keywords Doped ZnO · PSF membrane · Hydrophilicity · Salt rejection

1 Introduction

Polysulfone (PSf) membranes have been widely applied in various applications including biotechnology, pharmaceutical, and medical industries owing to their stability under different conditions [1]. The PSf membranes have superior thermal and chemical properties and are resistant to a high range of pH and temperature which makes them suitable to applied in separation and filtration processes [2]. In addition, the unique structure of PSf allows its membranes to exhibit high mechanical strength compared to other membranes, and it can be easily fabricated using phase inversion techniques [3]. One of the major drawbacks of PSf membranes is fouling which leads to a decrease in membrane permeability caused by hydrophobicity of membrane (or poor hydrophilicity) [4]. It was reported that the hydrophilicity of PSf membranes can be improved through blending them with metal oxides, organic, and inorganic nano-fillers [5]. In the past few years, several studies have focused on improving flux, mechanical strength, selectivity, and thermal resistance of PSf membranes by blending them with inorganic oxide nanoparticles (NPs) [6–8]. The addition of TiO_2 NPs to PSf membranes improved the hydrophilicity, pores number, water flux, and the mechanical strength [9]. It was also reported that adding SiO_2 NPs into PSf membrane can lead to the enlargement of the pores within the membranes, thus enhancing the water flux and reducing the fouling [10]. Furthermore, addition of magnetic NPs (Fe_3O_4) can enhance the water flux and improve salt rejection capabilities of the membranes [11]. Few studies have incorporated ZnO nanoparticles with PSf membranes and observed that the addition of nano-sized particles reduced the fouling of the membranes increasing water flux and made the membrane recyclable [12, 13]. Moreover, the addition of ZnO decorated on graphene oxide (GO) and GO-NiO blends to PSf

✉ Muneer M. Ba-Abbad
mbaabbad@qu.edu.qa

Nafis Mahmud
n.mahmud@qu.edu.qa

[1] Gas Processing Centre, College of Engineering, Qatar University, P.O. Box 2713, Doha, Qatar

[2] Department of Chemical and Process Engineering, Faculty of Engineering and Built Environment, Universiti Kebangsaan Malaysia, 43600 Bangi, Selangor, Malaysia

[3] Chemical and Water Desalination Program, College of Engineering, University of Sharjah, Sharjah 27272, United Arab Emirates

membranes has also reportedly improved the hydrophilicity and rejection performance of the membranes [14, 15]. It is evident from these studies that the performance of PSf membranes can be significantly improved through the incorporation of nanoparticles. Cobalt-based nanomaterials have been extensively applied to degrade organics from water, due to their higher activity [16–18]. Moreover, cobalt doped on zinc oxide has shown superior antibacterial activity against water-borne bacteria in comparison to pure ZnO nanoparticles [19]. Until now, there are limited studies on the effect of incorporating metal ions (like cobalt, Co^{2+}) doped ZnO NPs to enhance PSf membrane hydrophilicity. To the best of our knowledge, the effect of combining multifunctional Co^{2+}-doped ZnO NPs on improving of PSf membranes is not available in the open literature. In this work, Co^{2+}-doped ZnO NPs were synthesized using the sol-gel technique. The doped particles were combined with PSf membrane (ultrafiltration membranes) in order to improve PSf membrane properties such as hydrophilicity (contact angle), flux, porosity, and surface zeta potential. The pure and modified PSf membranes with 0.5 wt. % of ZnO and Co^{2+}-doped ZnO NPs were tested for salt rejection using sodium chloride (NaCl) and sodium sulfate (Na_2SO_4) as salts. The performance of all fabricated membranes was investigated using several techniques such as XRD, FESEM-EDX, TGA, AFM, and zeta potential.

2 Materials and methods

2.1 Materials

In this study, all membranes were prepared using polysulfone (PSf) pellets and solvent as N-methyl-2-pyrrolidone (NMP) were supplied from Good fellow Cambridge Ltd. (England) and Merck Company (Germany), respectively. The membrane rejection tests were performed using two different salts, namely, sodium chloride, and sodium sulfate both of which were purchased from R&M Chemicals.

2.2 Synthesized of doped ZnO NPs and membrane fabrication

The ZnO NPs with average crystal size of 18 ± 2 nm were synthesized under optimum condition through the sol-gel method [20]. The ZnO NPs were doped by 1.00 wt. % of Co^{2+} ions. The same conditions were used to prepare pure ZnO NPs. The average crystal size of doped ZnO NPs were14.3 ± 2 nm [21]. The simple technique as phase inversion was applied to prepare all PSf membranes. In case of the membranes doped with nanoparticles, fixed amount of either ZnO or doped ZnO NPs (0.50 wt. %) was incorporated in the final casting solution of PSf. Each casting solution consisted of 18 wt. % of PSf pellets was dissolved in the NMP solvent at 60 °C under stirring for 5 h. The blended membranes were prepared by adding the NPs into the PSf/NMP mixture according to ratios as summarized in Table 1.

Initially, both NPs were added in suitable amount of NMP in beakers and stirred for 4 h, and then, the mixtures were ultrasonicated for at least 30 min to avoid NP agglomeration. Final mixtures of NPs in NMP solution were added slowly into the PSf under vigorous stirring until homogeneous solutions were obtained. Furthermore, all mixtures of the homogenous solutions were ultrasonicated for 30 min to enhance of NP dispersion and degassed for 24 h. During the preparation of the membranes, small amount of the resultant NMP solution was poured onto the surface of the glass plate and dispersed using a Filmographe Doctor Blade and the final thickness of the membranes were 0.20 mm. After the casting process, the membranes were immediately immersed in water bath at ambient temperature to complete process of phase inversion.

2.3 Characterization of membranes

The crystallinity of pure and doped ZnO NPs along with the membranes were determined using X-ray diffractometer (Bruker D8 Advance AXS, Germany) with CuKα radiation ($\lambda = 1.5406$ Å) in the 2θ scan range of 5–80°. The thermal stability of the membranes was measured using the thermogravimetry analysis (STA 449F3, Jupiter, Netzsch, Germany) within range of 25 to 800 °C and rate of heating 10 °C/min. The hydrophilicity of membranes (contact angle) was measured by Easy Drop (Kurss) with ultrapure water as the media. The dead-end stirred cell with membrane surface area of 14.7 cm^2 (Sterlitech HP4750 stirred cell) was used to measure the membrane flux. The membranes were initially compacted for 1 h under the pressure of 10 bar. After that, the cell was filled with RO water to determine membrane permeate flux (J) by varying the pressure from 2 to 6 bars using the Eq. (1)

$$J = \frac{V}{(A \times t)} \tag{1}$$

where,

J: flux of permeate (L/m^2 h)

V: volume of permeate accumulative (L)

t: filtration time (h)

Table 1 Types of membrane based on polymer and nanoparticle ratios

Membrane type	PSf/NMP ratio (%)	NPs (wt. %)
PSf	18:82	0.00
PSf + ZnO NP	18:82	0.50
PSf + doped ZnO NP	18:82	0.50

A: membrane effective area the (0.00146 m^2)

The membrane porosity is very important test, which can be determine by gravimetric method as ratio between voids volume to the total membrane volume. The membrane was put in the oven for drying for 6 h at 50 °C, then weighted. The dried membrane pieces were submerged in distilled water for 24 h at room temperature. To remove any droplets on their surface, filter paper was used before any weight record was taken. Equation (2) was used to calculate the porosity (ε) [22].

$$\varepsilon = \frac{\omega_1 - \omega_2}{A \times l \times d_w} \tag{2}$$

where

ω_1, ω_2: weight of membranes as wet and dry (gm).

A: surface area of Membrane (m^2)

l: membrane thickness (m)

d_w: 998 kg/m^3 (density of water).

The surface morphology which includes the surface and cross-sectional of membranes was determined using a microscope with a Gemini model SUPRA 55VP-ZEISS, Oberkochen, of field emission scanning electron microscopy, Germany, with energy-dispersive X-ray spectroscopy (FESEM-EDX). The distribution of NPs on the membrane matrix was investigated by mapping images which was performed by Aztec version .3.0. Additionally, membrane roughness was evaluated using multimode atomic force microscopy (AFM, Bruker AXS, Corporation, Germany), with nanoscope IIIa controller (Veeco, USA). The dimension of each scanned membrane was 10 µm × 10 µm. The zeta potential of membrane is a main factor to investigate the surface charge, which influence on the flux and antifouling properties of membranes. Zeta potential of fabricated membranes was tested by the Malvern Zetasizer (model Nano-ZS). The piece of membrane with dimension 4 × 4 mm was used and immersed in 1 ml solution of mixture between latex stranded and sodium chloride (NaCl, 1 mM) with buffer of pH = 7.0. The rejection or prepared membranes for sodium chloride and sodium sulfate salts were determined using initial concentration of 20 mg/l (ppm). The rejections (*R*) were determined using Eq. (3)

$$R = \left(1 - \frac{C_p}{C_f}\right) \times 100 \tag{3}$$

where

C_f and C_p are feed and permeate concentration filtration (mg/l)

The concentration of sodium chloride and sodium sulfate salts before and after filtration was measured through the conductivity using Mettler Toledo's conductivity meter.

3 Results and discussion

3.1 XRD analysis

The XRD diffraction patterns of ZnO and doped ZnO NPs were presented in Fig. 1. Average crystal sizes of 18 and 14.3 nm were obtained for ZnO and doped ZnO NPs, respectively. The observed decrease in ZnO particle size by adding Co^{2+} ions was due to the smaller ionic radii of Co^{2+} (0.058 nm) compared to that of Zn^{2+} ions (0.074 nm) [21]. Hence, the presence of Co^{2+} ions inhibited the growth of the ZnO NP's which in turn resulted in the formation of smaller ZnO

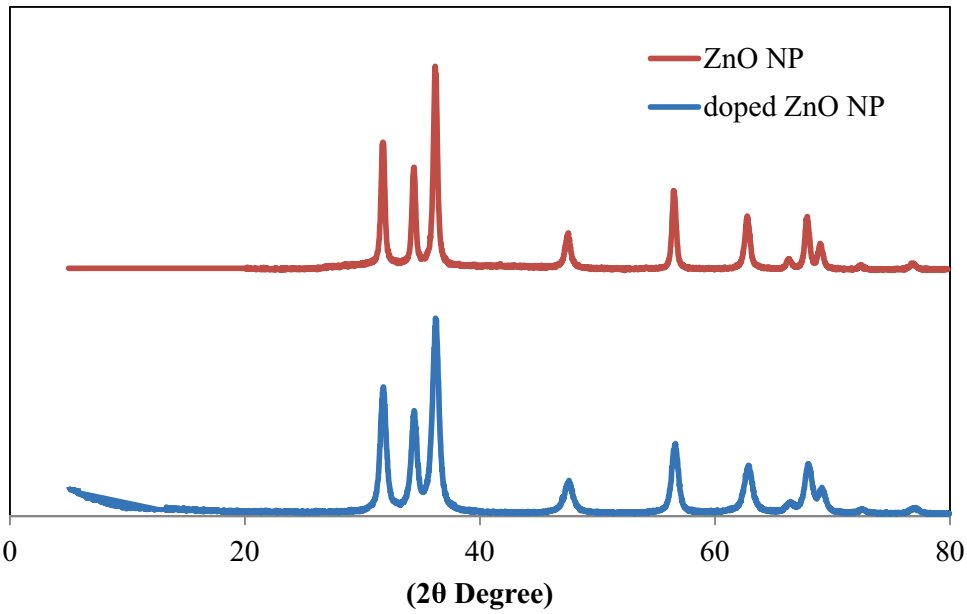

Fig. 1 The X-ray diffraction of synthesized ZnO and doped ZnO NPs

particles. However, inhibition of ZnO particles growth as a result of doping by Co^{2+} ions into the ZnO matrix was reported earlier [23]. Moreover, it can be seen that ZnO and doped ZnO NP powders have peaks at different 2θ values of 31.6, 34.3, 36.18, and 56.5 corresponding to the (100), (002), (101), and (110) plane, respectively, which confirms that the phase belongs to ZnO [23]. On the other side, composite membranes of PSf with ZnO NP and doped ZnO NP did not show any peak; the same behavior was observed for pure PSf membrane. The addition of NP to PSf membrane led to a decrease in the intensity of PSf membrane as observed in Fig. 2, which affirms the uniform dispersion of NPs in the membrane matrix. This behavior was more profound within the doped ZnO samples owing to the good interaction between the NPs [24] and the PSf matrix. Lower amount and well distribution of both NPs were considered to be the main factor for the peak of NPs which was not detected in the PSf diffraction pattern as reported earlier[25].

3.2 Thermal property

The stability of fabricated membranes was investigated by thermogravimetry analysis (TGA) with a temperature range of 26 to 800 °C. Three weight losses of PSf membranes incorporated with ZnO and doped ZnO NPs were found in Fig. 3. The first weight loss shows after 100 °C, which is referred to desorption of adsorbed water and residual solvent in membrane structure. After 500 °C, two weight losses

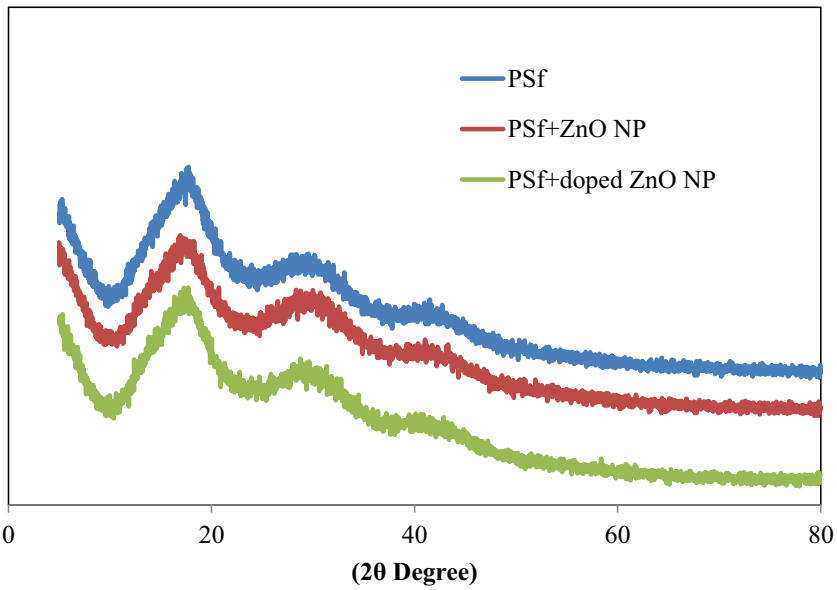

Fig. 2 The X-ray diffraction of PSf membranes incorporated with ZnO and doped ZnO NPs

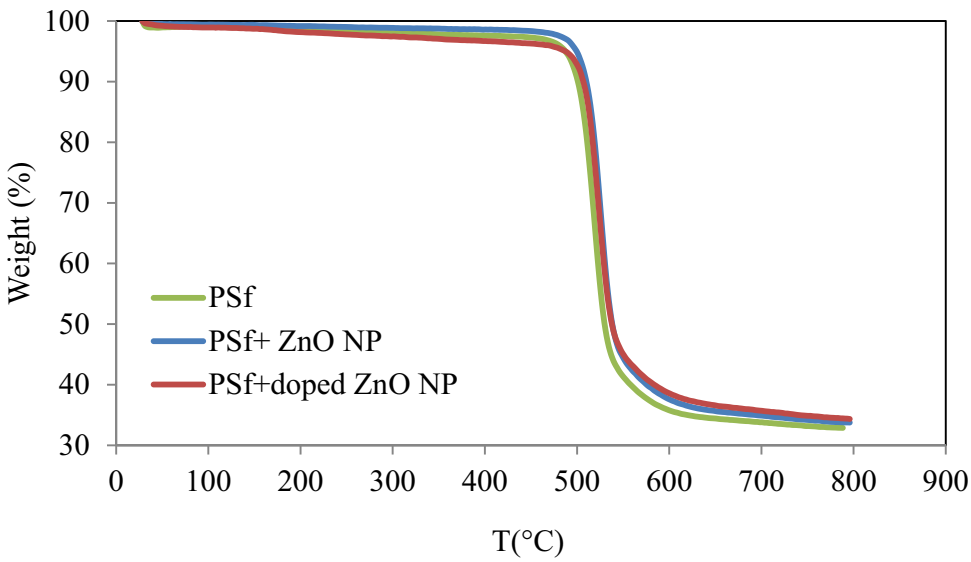

Fig. 3 Thermal decomposition of fabricated membranes

were observed which were related to degradation of polymer chains. However, PSf membranes with embedded ZnO and doped ZnO NPs show slightly improved of thermal stability compared to pure PSf membranes [26]. The first derivative peak of the PSf blended with both ZnO and doped ZnO membranes appeared at 543 ± 0.5 °C while that of pure PSf membrane at 533 ± 0.5 °C. The blended membranes showed slightly higher weight loss and they were to be 65, 63.34, and 61.67% for PSf and blended with both ZnO and doped ZnO membranes, respectively.

This results attributed to a more homogeneous dispersion of both ZnO and doped ZnO NPs with low amount in the casting solution of PSf [27]. The enhancement of the thermal stability of PSf blended membrane maybe attributed to the NPs acting as thermal blocker against heat diffusion, and the covalent bonds formed between the PSf and NPs [28]. Therefore, these results further confirm that ZnO and doped ZnO NPs were uniformly dispersed into the matrix of PSf membrane.

3.3 Morphology analysis

Figure 4 shows the structure of PSf membrane blended with ZnO and doped ZnO NPs represented by surface and cross-section images obtained from FESEM with EDX analysis. The structure of the three types of studied membranes showed a typical asymmetric morphology with finger-like pores linked by sponge walls. The presence of NPs did not bring any changes in the membrane morphology compared to pure PSf membrane as presence in Figure 4. The surface of all the membranes were smooth and flat faced without any trace of NPs.

The FESEM images indicated that the membrane structure was improved by the incorporation of ZnO and doped ZnO NPs compared to the pure PSf membranes. This

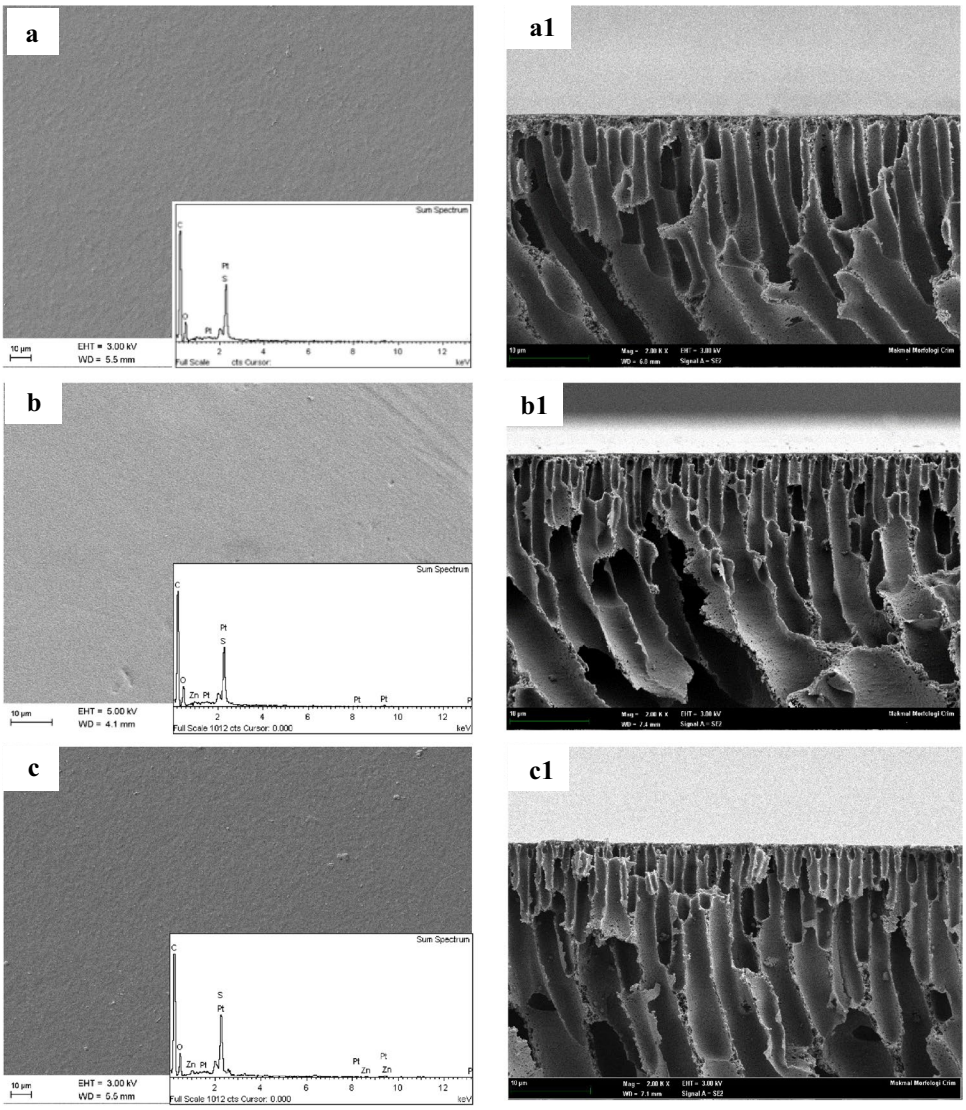

Fig. 4 Surface and cross-section analysis using FESEM for (a, a1) PSf, (b, b1) PSf + ZnO NP, and (c, c1) PSf + doped ZnO NP membranes

phenomenon indicated that ZnO and doped ZnO NP dispersed uniformly into the membrane with lower agglomerations [29]. Therefore, clearly the pores were well distributed on the surface of PSf membrane with NPs due to the reduction of interfacial stresses between NPs and PSf polymer during the drying stage of membrane [30]. To determine the composition of the PSf membrane before and after blending it with NPs, the EDX measurement was performed. Clearly, it can be observed that only C and S peaks were detected in pure PSf membrane, while an additional peak for Zn was observed for ZnO and doped ZnO NP-modified PSf membranes as shown in Fig. 4. This element composition analysis was further investigated by EDX mapping to confirm of these NPs in the matrix of the membranes [30]. Fig. 5 shows good distribution of both additive ZnO and doped ZnO NP in the PSf membranes. Fig. 5 b and c represents the distribution of ZnO and doped ZnO NP in the PSf membrane, respectively. Very low distribution of Co^{2+} was obtained for doped ZnO NP-modified PSf membrane which was attributed to the lower concentration (1.0 wt. %) of Co^{2+} ions used.

The surface morphology of the pure PSf and blended it with ZnO, and doped ZnO NPs were evaluated by AFM analysis. The 3D images (three dimensional) of the samples are presented in Fig. 6. Two different surface area on membrane were observed as bright and dark areas, which represents the highest points and pores of membrane, respectively.

The AFM analysis of modified PSf membranes by NPs focusses on average surface roughness (R_a) and root mean square roughness (R_q) as given Table 2, and it was found to be lower in comparison with PSf membranes. These results are an indication of the partial blockage of the pores on the membrane surface by ZnO and doped ZnO NPs leading to reduced pore radius on the membrane surface. This reduction of blended membrane pore size leads to the formation of smoother surface as reported in the previous study [31]. Based on this fact, any increase in the amount of NP additives caused an increase in the surface roughness by the agglomerated of the NPs on the surface of membrane as reported earlier[32]. Additionally, the smoother surfaces showed reduce of irreversible attachment between the foulants and membrane top surface that leads to increase of water flux [33].

3.4 Membrane hydrophilicity, water flux, and porosity

The contact angle, water flux, and porosity membranes of PSf and PSf with ZnO, and doped ZnO NPs are illustrated in Fig. 7. The low contact angle observed for the membranes attributes to higher hydrophilicity [33]. From the results, an obvious decline of the contact angle of the membrane blended with ZnO to doped ZnO NPs compared to non-additive PSf membrane was observed.

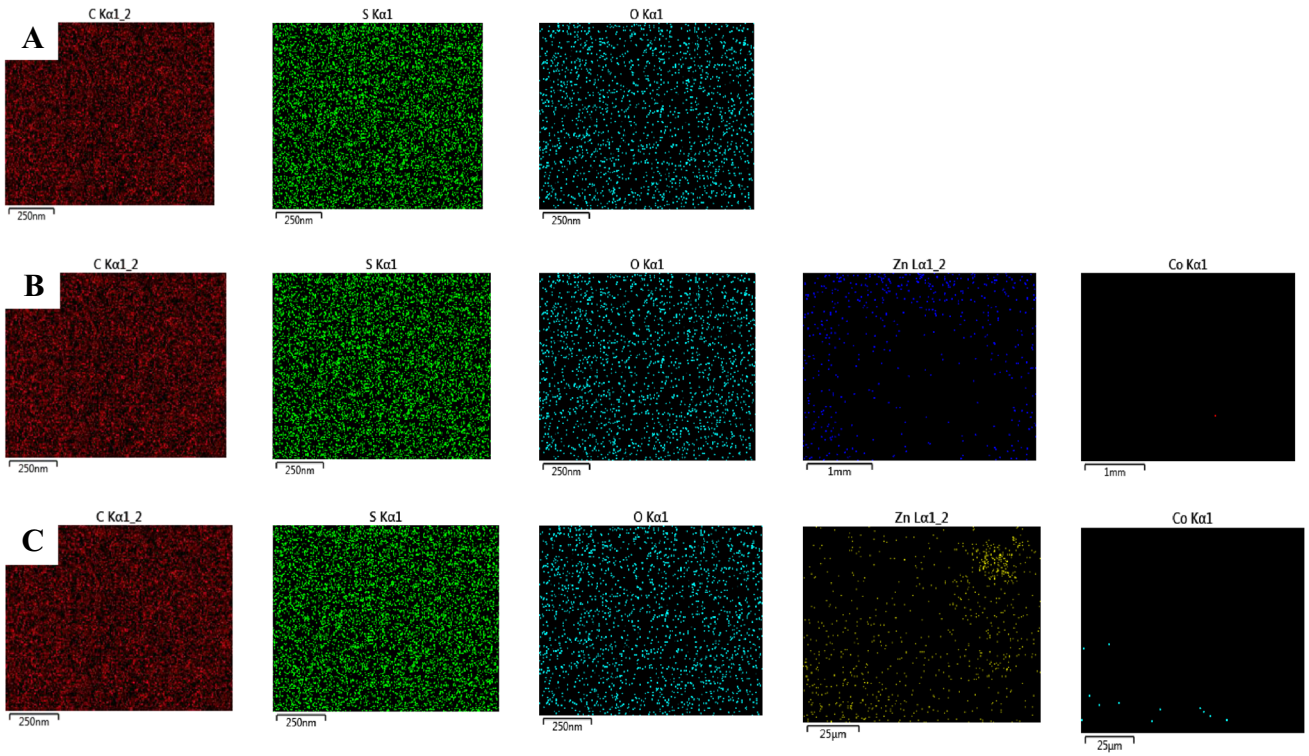

Fig. 5 Mapping of element distribution of membranes **A** PSf, **B** PSf + ZnO NP, and **C** PSf + doped ZnO NP

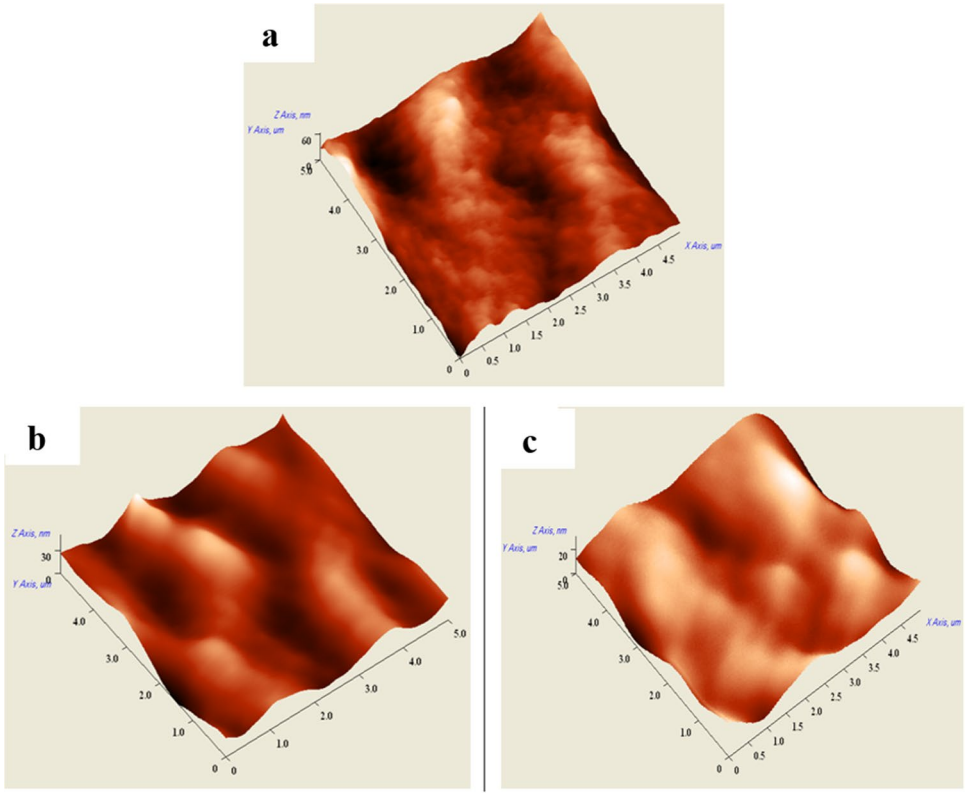

Fig. 6 AFM analysis with 3D images of membrane surface morphology **a** PSf, **b** PSf + ZnO NP, and **c** PSf + doped ZnO NP

Table 2 Roughness parameters of membrane surface

Membrane type	Mean surface roughness R_a (nm)	Root mean square roughness R_q (nm)
PSf	8.056	10.158
PSf + ZnO NP	5.636	6.943
PSf +doped ZnO NP	3.364	4.246

The contact angle value was found to be as 82.7 ± 0.9 for pure PSf membrane. Addition of 0.5 wt. % of ZnO and doped ZnO NP, brought about a remarkable decrease of the membrane contact angle from 82.7 ± 0.9 to 75.4 ± 0.52 and 62.4± 0.35 respectively. The addition of small amount (0.5 wt%) of doping improved the membrane hydrophilicity compared to pure PSf membranes. This improvement on hydrophilicity is attributed to effected by reducing interface energy of the membranes matrix by ZnO NPs polarity and modified polarity by doped Co^{2+} ions in ZnO matrix and increased surface area [34].

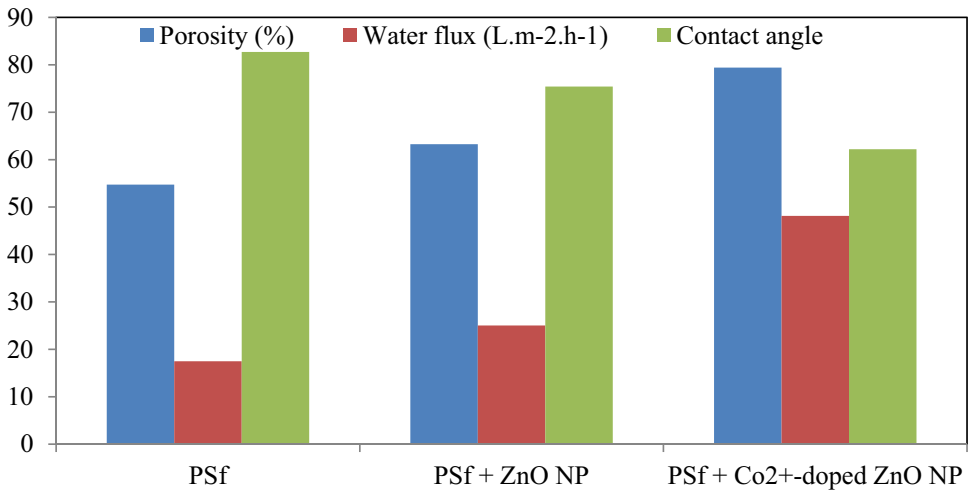

Fig. 7 Effect of ZnO and doped ZnO NPs blended PSf on membrane properties

Therefore, the hydrophilicity of hybrid membranes with NPs directly affected the water flux of membrane as shown in Fig. 7. However, increasing of water flux from 17.49 to 25.03 and 48.14 L m^{-2} h^{-1} for pure PSf, ZnO, and doped ZnO NP PSf membranes respectively. This phenomena of solvent and non-solvent exchange rate within the fabrication of membrane by phase inversion were significant factors in enhancing the membrane flux [34]. Blend of ZnO and doped ZnO NPs with PSf casting solution caused the reduction of solution viscosity, which attributed to hydrophilic property of NPs that can increase rate exchange of solvent with non-solvent such as NMP and water, respectively [35]. This result shows a good enhancement of diffusion rate under lower viscous blending of solution which could increase of membrane permeability [35].

In general, the porosity result of a hybrid PSf membrane with both NPs showed a higher comparison to pure PSf in the study reported earlier [36]. However, phase inversion process factors such as mass transfer can control the membrane porosity during the preparation stage [37]. In this study, the hydrophilic property of the ZnO NPs showed a significant effect on the porosity hybrid membrane. The increase in porosity of the hybrid PSf membrane with both NPs was because of the enhancement of pores formation by exchange rate increase for the non-solvent and solvent in the presence of NPs [38]. Increasing pure PSf membrane porosity (54.74%) up to 63.27% and 79.442% for the blend with ZnO and doped ZnO NP membranes, respectively, were observed.

3.5 Membrane zeta potential

The membrane surface property is an important factor to study in relation to other factors such as antifouling and flux of membranes [39]. The zeta potential analysis of the membrane surface incorporated with ZnO and doped ZnO NPs was measured and is shown in Fig. 8. From the results, it can be observed that all values for pure PSf, ZnO, and doped ZnO hybrid PSf membranes are negative. However, a higher negative value of − 19.34 was found for doped ZnO NPs hybrid PSf membrane and followed by − 10.56 and − 6.45 for ZnO NPs hybrid PSf and pure PSf membranes, respectively. These results could be explained by the natural migration of the more hydrophilic ZnO and doped ZnO to the PSf membrane surface increasing negative charge of the surface [27–29, 39]. The highest negative value obtained with doped ZnO hybrid PSf led to the increase of surface area (smaller particle size) with lower agglomeration of doped ZnO NPs as observed from XRD analysis.

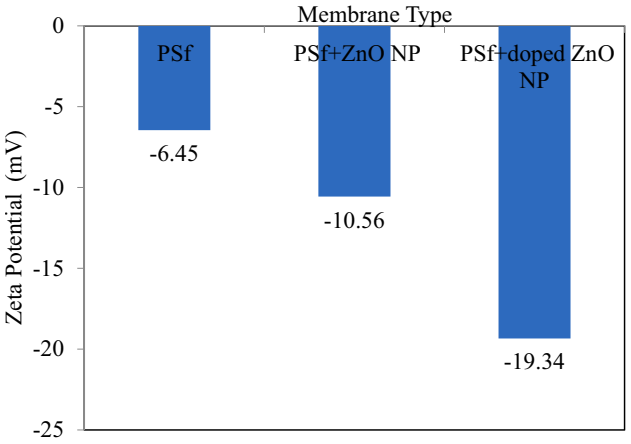

Fig. 8 Zeta potential of fabricated PSf surface membranes with ZnO and doped ZnO NP

3.6 Validation of hydrophilicity using nanoparticles

The hydrophilicity of the hybrid ZnO and doped ZnO NP PSf membranes was compared with the results for other hybrid PSf membranes reported in the literature and summarized in Table 3. Polyether-sulfone (PES) membranes were also included in this comparison since they exhibit similar behavior to those PSf membranes [38]. It can be clearly seen that even small addition of the NPs showed significant improvement even when using a very small amount of 0.50 wt. % blended with the membrane solution. However, the majority of other investigators as shown in Table 3 used different copolymers such as polyethylene glycol (PEG), polyvinylpyrrolidone (PVP), polyvinyl alcohol (PVA), and chitosan (CH) at varying weight blended with membrane in the presence of NPs. These copolymers help to improve the hydrophilicity of PSf membranes owing to their hydrophilic nature [47]. Only a few studies have reported using NP doping as low as 0.50 wt % in their investigation and most of the studies used a doping of more than 1.00 wt%. In this work, only 0.5 wt% NPs of Co^{2+}-doped ZnO NP were used to modify the hydrophilicity (Reduction of contact angle, Rca%) of the PSf membranes and this is being reported for the first time for Co^{2+}-doped ZnO NP, hence, the results were compared with other membranes with similar amounts of nanomaterials doping available in the literature (Table 3). The R_{ca} % using ZnO hybrid PSf membrane showed results close to other membranes blended with NPs such as TiO_2, SiO_2, and graphene oxide (GO). However, membranes blended ZnO NPs in the presence of copolymer resulted in much higher improvement of R_{ca} % compared to other NPs of TiO_2 and SiO_2 which referred to a higher surface area [40–45]. Recently, graphitic carbon nitrides (g-C_3N_4) nanocomposite as carbon-based NPs incorporated with ZnO NPs showed good result of R_{ca} % without any copolymer due to decreases of ZnO aggregation [46]. The R_{ca} % of PSf hybrid doped ZnO NPs

Table 3 Comparison of hydrophilicity of PSf and PES membranes blended with different types of nanoparticles

Type of NPs	Type of membrane with copolymer (%)	Amount of additive (wt. %)	Reduction of contact angle (R_{ca} %)	Contact angle range (°)	References
TiO_2	PES	0.50	8	75 to 68	[40]
SiO_2	PSf	0.50	10.2	75.42 to 67.75	[10]
GO	PSf	0.50	5.0	75.42 to 71.6	[10]
GO	PES + CH	0.50	7.3	87.4 to 81.0	[2]
ZnO	PES + PVP, 1.7	0.50	16.6	66.5 to 54.8	[33]
ZnO	PES + PEG, 2	0.50	9.8	79.9 to 72.0	[41]
ZnO	PES + PVP, 2	0.50	11.2	75.5 to 66.9	[42]
ZnO	PVC+ PEG	1.0	8.0	67.5 to 62.1	[43]
ZnO-GO	PSf	1.0	2.8	77.2 to 75.0	[44]
ZnO	PSf + DME + PVP	1.0	7.9	63.0 to 58.0	[45]
g-C_3N_4/ZnO	PSf	0.5	21.5	65.3 to 51.2	[46]
ZnO	PSf	0.50	8.9	82.7 to 75.4	This study
Co^{2+}-doped ZnO	PSf	0.50	24.7	82.7 to 62.2	This study

gives highest value of about 24.7% using the amount of 0.5 wt. % without adding any copolymer. These results indicated that modified ZnO NPs by doping Co^{2+} ions could have appreciable economical results in the area of membrane applications by reducing the fouling phenomena and membrane cost. There is also scope of further improvement in the performance of the Co^{2+}-doped ZnO NPs through the addition of copolymers.

3.7 Performance of membrane for salt rejection

The rejection performance of PSf and hybrid with ZnO NPs and Co^{2+} ions doped ZnO NPs membranes were evaluated using two types of salt solution namely sodium chloride (NaCl) and sodium sulfate (Na_2SO_4). From Fig. 9, both of ZnO and doped ZnO NPs hybrid PSf membranes exhibited higher salt rejections for both salts compared to pure PSf membrane. The hybrid PSf membranes indicated almost similar rejection tendency for both salts. More importantly, both hybrid PSf membranes demonstrated higher flux as well as higher rejection of salts. This result indicates that the addition of small amount of ZnO and doped ZnO NPs into the PSf matrix can result in an improvement of hydrophilicity of pure PSf membrane, thus, resulting in more flux through the membrane surface [45]. This improvement also leads to a reduction of antifouling behavior (enhancing the fouling resistance), which can reduce the adsorption of organic pollutants on the membrane surface as reported earlier [27, 46]. Thus, the contribution of the negative charged ions for both salt ions, i.e., Cl^- and SO_4^{2-} to the modified charge of membrane surface is negated by the presence of both NPs leading to the increase in Donnan repulsion [48]. Hence, the highly hydrophilic structure of the ZnO NP-doped hybrid membranes could significantly enhance

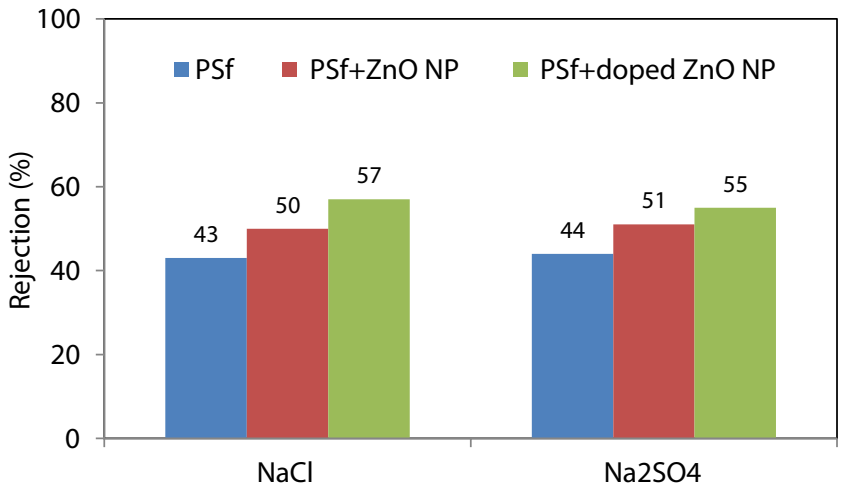

Fig. 9 Performance of fabricated PSf with ZnO and doped ZnO NP membranes for both salt rejections

the salt rejection capacity and this makes them an excellent candidate for water purification applications.

4 Conclusion

Both pure and Co^{2+} ions doped ZnO NPs were blended with PSf to prepare of different membranes through the simple phase inversion technique. The results showed that doping Co^{2+} ions on ZnO NPs could significantly improve the zeta potential, which in turn enhanced the hydrophilicity and water flux of PSf membranes. The addition of doped ZnO NP in the PSf membrane also resulted in a reduced contact angle, which also improved the membrane porosity and pure water flux. Furthermore, the doped ZnO PSf membranes exhibited higher salt rejection behavior affirming the advantage of having Co^{2+} doping with ZnO NPs and embedded with PSf membranes. Overall, the results obtained from this study clearly demonstrate the exceptional properties of Co^{2+} ions doped ZnO NP which can significantly improve PSf membrane properties in terms of its hydrophilicity, and it can also further reduce its fouling behavior. Based on these results, it can be suggested that the unique properties of prepared Co^{2+} ions doped ZnO NPs make them a suitable candidate for membrane modification and industrial applications in future.

Acknowledgements The authors would like to acknowledge the technical support of the Central Laboratories Unit (CLU), Qatar University and Centre for Research and Instrumentation Management (CRIM), Universiti Kebangsaan Malaysia, in performing the analysis.

Author contribution All authors have equal contributions. All authors have read and agreed to the published version of the manuscript.

Funding Open Access funding provided by the Qatar National Library. Open Access funding provided by the Qatar National Library.

Declarations

Conflict of interest The authors declare no competing interests.

References

1. A.M. Pandele, M. Oprea, A.A. Dutu, F. Miculescu, S.I. Voicu, A novel generation of polysulfone/crown ether-functionalized reduced graphene oxide membranes with potential applications in hemodialysis. Polymers **14**(1), 148 (2021)
2. A.T. Yasir, A. Benamor, A.H. Hawari, E. Mahmoudi, Graphene oxide/chitosan doped polysulfone membrane for the treatment of industrial wastewater. Emergent Mater, **6**, 899–910. https://doi.org/10.1007/s42247-023-00504-0 (2023)
3. H. Wei, W. Wang, X. Xie, Z. Shu, Z. Yi, C. Gao, Highly cross-linked, nanoporous polysulfone/MOFs mixed matrix membranes with excellent resistance to harsh solvents with strong polarity. Polymer **275**, 125927 (2023)
4. M. El Batouti, N.F. Alharby, M.M. Elewa, Review of new approaches for fouling mitigation in membrane separation processes in water treatment applications. Separations **9**(1), 1 (2021)
5. C. Wang, B. Lin, Y. Qiu, Enhanced hydrophilicity and anticoagulation of polysulfone materials modified via dihydroxypropyl, sulfonic groups and chitosan. Colloids Surf B: Biointerfaces **210**, 112243 (2022)
6. M. Khraisheh, S. Elhenawy, F. AlMomani, M. Al-Ghouti, M.K. Hassan, B.H. Hameed, Recent progress on nanomaterial-based membranes for water treatment. Membranes **11**(12), 995 (2021)
7. A. Bedar, D. Yadav, S. Kriti, R.K. Das, S. Saxena, S. Shukla, Nanomagnets doped antifouling membrane for fine emulsion separation. Polymer **290**, 126484 (2024)
8. H. Abdallah, S. Gaballah, M.S. Mansour, H. Farag, Y.H. Farid, Separation of diclofenac sodium using polysulfone membranes incorporated with manganese nanoparticles. Chem Eng Technol **46**(4), 600–613 (2023)
9. S.H. Salim, R.H. Al-Anbari, A. Haider, Polysulfone/TiO2 thin film nanocomposite for commercial ultrafiltration membranes. J Appl Sci Nanotechnol **2**(1), 80–89 (2022)
10. T.D. Kusworo, A.C. Kumoro, N. Aryanti, D.P. Utomo, H. Hasbullah, F.F. Lingga, A. Widiastuti, M. Yulfarida, F. Dalanta, T.A. Kurniawan, Photocatalytic antifouling nanohybrid polysulfone membrane using the synergetic effect of graphene oxide and SiO2 for effective treatment of natural rubber-laden wastewater. J Membr Sci **657**, 120663 (2022)
11. M. Nasir, Y. Purnama Utami, N. Faaizatunnisa, L. Rohmawati, E. Suebah, A. Taufiq, E.S. Sazali, The GO-Fe3O4/Psf membrane prepared by phase inversion for filtration: Dyes and NaCl in water, Journal of Water and Environmental. Nanotechnology **8**(3), 241–253 (2023)
12. T.D. Kusworo, A.C. Kumoro, N. Aryanti, T.A. Kurniawan, F. Dalanta, N.H. Alias, Photocatalytic polysulfone membrane incorporated by ZnO-MnO2@ SiO2 composite under UV light irradiation for the reliable treatment of natural rubber-laden wastewater. Chem Eng J **451**, 138593 (2023)
13. L. Shen, Z. Huang, Y. Liu, R. Li, Y. Xu, G. Jakaj, H. Lin, Polymeric membranes incorporated with ZnO nanoparticles for membrane fouling mitigation: A brief review. Front Chem **8**, 224 (2020)
14. O.T. Mahlangu, G. Mamba, B.B. Mamba, A facile synthesis approach for GO-ZnO/PES ultrafiltration mixed matrix photocatalytic membranes for dye removal in water: Leveraging the synergy between photocatalysis and membrane filtration. J Environ Chem Eng **11**(3), 110065 (2023)
15. A. Maqbool, A. Shahid, Z. Jahan, M.B.K. Niazi, M.A. Inam, A.M. Tawfeek, E.M. Kamel, M.S. Akhtar, Development of ZnO-GO-NiO membrane for removal of lead and cadmium heavy metal ions from wastewater. Chemosphere **338**, 139622 (2023)
16. A. Anele, S. Obare, J. Wei, Recent trends and advances of Co3O4 nanoparticles in environmental remediation of bacteria in wastewater. Nanomaterials **12**(7), 1129 (2022)

17. Q. Gao, G. Wang, Y. Chen, B. Han, K. Xia, C. Zhou, Utilizing cobalt-doped materials as heterogeneous catalysts to activate peroxymonosulfate for organic pollutant degradation: a critical review. Environ Sci Water Res **7**(7), 1197–1211 (2021)
18. W. Zhao, Q. Shen, T. Nan, M. Zhou, Y. Xia, G. Hu, Q. Zheng, Y. Wu, T. Bian, T. Wei, Cobalt-based catalysts for heterogeneous peroxymonosulfate (PMS) activation in degradation of organic contaminants: Recent advances and perspectives. J Alloys Compd **958**, 170370(2023)
19. S. Gouthamsri, K. Jaya Rao, M. Ramanaiah, K. Basavaiah, Combustion-mediated sol–gel preparation of cobalt-doped ZnO nanohybrids for the degradation of acid red and antibacterial performance, Open. Chemistry **21**(1), 20230129 (2023)
20. M.M. Ba-Abbad, A.A.H. Kadhum, A.B. Mohamad, M.S. Takriff, K. Sopian, The effect of process parameters on the size of ZnO nanoparticles synthesized via the sol–gel technique. J Alloys Compd **550**, 63–70 (2013)
21. M.M. Ba-Abbad, M.S. Takriff, A. Benamor, A.W. Mohammad, Synthesis and characterisation of Co2+-incorporated ZnO nanoparticles prepared through a sol-gel method. Adv Powder Technol **27**(6), 2439–2447 (2016)
22. O. Serbanescu, S. Voicu, V. Thakur, Polysulfone functionalized membranes: Properties and challenges. Mater Today Chem **17**, 100302 (2020)
23. K. Singh, H. Kaur, P.K. Sharma, G. Singh, J. Singh, ZnO and cobalt decorated ZnO NPs: Synthesis, photocatalysis and antimicrobial applications. Chemosphere **313**, 137322 (2023)
24. P. Peechmani, M.H.D. Othman, R. Kamaludin, M.H. Puteh, J. Jaafar, M.A. Rahman, A.F. Ismail, S.H.S.A. Kadir, R.M. Illias, J. Gallagher, High flux polysulfone braided hollow fiber membrane for wastewater treatment role of zinc oxide as hydrophilic enhancer. J Environ Chem Eng **9**(5), 105873 (2021)
25. R. Rajakumaran, M. Kumar, R. Chetty, Morphological effect of ZnO nanostructures on desalination performance and antibacterial activity of thin-film nanocomposite (TFN) membrane. Desalination **495**, 114673 (2020)
26. H.Y. Phin, J.C. Sin, S.H. Tan, T.L. Chew, Y.T. Ong, Fabrication of asymmetric zinc oxide/carbon nanotubes coated polysulfone photocatalytic nanocomposite membrane for fouling mitigation. J Appl Polym Sci **138**(40), 51194 (2021)
27. E. Mahmoudi, L. Ng, A. Mohammad, M. Ba-Abbad, Z. Razzaz, Enhancement of polysulfone membrane with integrated ZnO nanoparticles for the clarification of sweetwater. Int J Environ Sci Technol **15**, 561–570 (2018)
28. Y. Jafarzadeh, R. Yegani, M. Sedaghat, Preparation, characterization and fouling analysis of ZnO/polyethylene hybrid membranes for collagen separation. Chem Eng Res Des **94**, 417–427 (2015)
29. R. Rajakumaran, V. Boddu, M. Kumar, M.S. Shalaby, H. Abdallah, R. Chetty, Effect of ZnO morphology on GO-ZnO modified polyamide reverse osmosis membranes for desalination. Desalination **467**, 245–256 (2019)
30. K. Pusphanathan, H. Shukor, N.F. Shoparwe, M.M.Z. Makhtar, N.I. Zainuddin, N. Jullok, M.R. Siddiqui, M. Alam, M. Rafatullah, Efficiency of fabricated adsorptive polysulfone mixed matrix membrane for acetic acid separation. Membranes **13**(6), 565 (2023)
31. V. Vatanpour, G.N. Nekouhi, M. Esmaeili, Preparation, characterization and performance evaluation of ZnO deposited polyethylene ultrafiltration membranes for dye and protein separation. J Taiwan Inst Chem Eng **114**, 153–167 (2020)
32. K. Szymański, D. Darowna, P. Sienkiewicz, M. Jose, K. Szymańska, M. Zgrzebnicki, S. Mozia, Novel polyethersulfone ultrafiltration membranes modified with Cu/titanate nanotubes. J Water Process Eng **33**, 101098 (2020)
33. S. Zhao, W. Yan, M. Shi, Z. Wang, J. Wang, S. Wang, Improving permeability and antifouling performance of polyethersulfone ultrafiltration membrane by incorporation of ZnO-DMF dispersion containing nano-ZnO and polyvinylpyrrolidone. J Membr Sci **478**, 105–116 (2015)
34. Y.-J. Li, G.-E. Chen, H.-Y. Xie, Z. Chen, Z.-L. Xu, H.-F. Mao, Increasing the hydrophilicity and antifouling properties of polyvinylidene fluoride membranes by doping novel nano-hybrid ZnO@ZIF-8 nanoparticles for 4-nitrophenol degradation. Polym Test **113**, 107613 (2022)
35. Z. Arif, N. Sethy, P. Mishra, B. Verma, Development of eco-friendly, self-cleaning, antibacterial membrane for the elimination of chromium (VI) from tannery wastewater. Int J Environ Sci Technol **17**, 4265–4280 (2020)
36. O.M. Shahlol, H. Isawi, M.G. El-Malky, A.E.-H.M. Al-Aassar, Performance evaluation of the different nano-enhanced polysulfone membranes via membrane distillation for produced water desalination in Sert Basin-Libya. Arab J Chem **13**(4), 5118–5136 (2020)
37. C. Bărdacă Urducea, A.C. Nechifor, I.A. Dimulescu, O. Oprea, G. Nechifor, E.E. Totu, I. Isildak, P.C. Albu, S.G. Bungău, Control of nanostructured polysulfone membrane preparation by phase inversion method. Nanomaterials **10**(12), 2349 (2020)
38. S. Zhang, H. Yuan, C. Wang, X. Liu, J. Lu, Antifouling performance enhancement of polyethersulfone ultrafiltration membrane through increasing charge-loading capacity over Prussian blue nanoparticles. J Appl Polym Sci **137**(45), 49410 (2020)
39. H. Mohamed, S. Hudziak, V. Arumuganathan, Z. Meng, M.-O. Coppens, Effects of charge and hydrophilicity on the anti-fouling properties of kidney-inspired, polyester membranes. Mol Syst Des Eng **5**(7), 1219–1229 (2020)
40. A. Sotto, A. Boromand, R. Zhang, P. Luis, J.M. Arsuaga, J. Kim, B. Van der Bruggen, Effect of nanoparticle aggregation at low concentrations of TiO2 on the hydrophilicity, morphology, and fouling resistance of PES–TiO2 membranes. J Colloid Interface Sci **363**(2), 540–550 (2011)
41. L. Shen, X. Bian, X. Lu, L. Shi, Z. Liu, L. Chen, Z. Hou, K. Fan, Preparation and characterization of ZnO/polyethersulfone (PES) hybrid membranes. Desalination **293**, 21–29 (2012)
42. X. Li, J. Li, B. Van der Bruggen, X. Sun, J. Shen, W. Han, L. Wang, Fouling behavior of polyethersulfone ultrafiltration membranes functionalized with sol–gel formed ZnO nanoparticles. RSC Adv **5**(63), 50711–50719 (2015)
43. H. Rabiee, V. Vatanpour, M.H.D.A. Farahani, H. Zarrabi, Improvement in flux and antifouling properties of PVC ultrafiltration membranes by incorporation of zinc oxide (ZnO) nanoparticles. Sep Purif Technol **156**, 299–310 (2015)
44. N.A. Rosnan, Y. Teow, A.W. Mohammad, The effect of ZnO loading for the enhancement of PSF/ZnO-GO mixed matrix membrane performance. Sains Malays **47**, 2035–2045 (2018)
45. R. Rezaee, R. Rahimipour, A. Maleki, M. Safari, B. Shahmoradi, A. Jafari, S.A. Mousavi, Evaluation of a nanohybrid membrane (PSF/ZnO) efficiency in natural organic matter removal from water. J Adv Environ Health Res **10**(3), 253–262 (2022)
46. V. Vatanpour, S.S. Mousavi Khadem, A. Dehqan, S. Paziresh, M.R. Ganjali, M. Mehrpooya, E. Pourbasheer, A. Badiei, A. Esmaeili, I. Koyuncu, G. Naderi, N. Rabiee, O. Abida, S. Habibzadeh, M.R. Saeb, Application of g-C3N4/ZnO nanocomposites for fabrication of anti-fouling polymer membranes with dye and protein rejection superiority. J Membr Sci **660**, 120893 (2022)
47. N. Gan, Y. Lin, Y. Zhang, V. Gitis, Q. Lin, H. Matsuyama, Surface mineralization of the TiO2–SiO2/PES composite membrane with outstanding separation property via facile vapor-ventilated in situ chemical deposition. Langmuir **38**(42), 12951–12960 (2022)
48. C. Hu, Z. Liu, X. Lu, J. Sun, H. Liu, J. Qu, Enhancement of the Donnan effect through capacitive ion increase using an electroconductive rGO-CNT nanofiltration membrane. J Mater Chem A **6**(11), 4737–4745 (2018)